

Distinct interleukin-6 production in IPL and TAFRO subtypes of idiopathic multicentric Castleman disease

Asami Nishikori,¹ Midori Filiz Nishimura,¹ Yoshito Nishimura,² Rio Yamada,¹ Tomoka Haratake,¹ Daisuke Ennishi,^{3,4} Ryota Chijimatsu,³ Toshihiro Ito,⁵ Tomohiro Koga,⁶ Sayaka Ochi,¹ Yuri Kawahara,¹ Himawari Ueta,¹ Yudai Takeda,¹ Michael V. Gonzalez,⁷ David C. Fajgenbaum,^{7,8} Frits van Rhee,⁹ Shuji Momose¹⁰ and Yasuharu Sato^{1*}

¹Department of Molecular Hematopathology, Okayama University Graduate School of Health Sciences, Okayama, Japan; ²Division of Hematology/Oncology, Mayo Clinic, Rochester, MN, USA; ³Center for Comprehensive Genomic Medicine, Okayama University Hospital, Okayama, Japan; ⁴Department of Hematology and Oncology, Okayama University Hospital, Okayama, Japan; ⁵Department of Immunology, Nara Medical University, Nara, Japan; ⁶Department of Immunology and Rheumatology, Nagasaki University Graduate School of Biomedical Sciences, Nagasaki, Japan; ⁷Center for Cytokine Storm Treatment & Laboratory, Department of Medicine, Perelman School of Medicine, University of Pennsylvania, Philadelphia, PA, USA; ⁸Castleman Disease Collaborative Network, Philadelphia, PA, USA; ⁹University of Arkansas for Medical Sciences, Little Rock, AR, USA and ¹⁰Department of Pathology, Saitama Medical Center, Saitama Medical University, Saitama, Japan

Correspondence: Y. Sato
satou-y@okayama-u.ac.jp

Received: May 6, 2025.

Accepted: August 29, 2025.

Early view: September 11, 2025.

<https://doi.org/10.3324/haematol.2025.288147>

©2026 Ferrata Storti Foundation

Published under a CC BY-NC license



Supplementary Methods

Immunohistochemistry, sample quantification, and In situ hybridization

Immunohistochemical staining was performed on an automated Bond-III instrument (Leica Biosystems, Wetzlar, Germany) using the primary antibody of IL-6 (10C12, 1:200, Leica Biosystems). Internal positive and negative control cells were confirmed. The slides were scanned using a Nanozoomer whole-slide scanner (Hamamatsu Photonics, Hamamatsu, Japan) at 40X magnification and analyzed using QuPath (version 0.4.3, University of Edinburgh, UK). Single-cell detection was performed using QuPath. Each cell was scored from 0 (negative) to 3 (strongly positive) according to diaminobenzidine intensity, and the H-score was calculated. The H-score was calculated for cell staining using the following formula: $H\text{-score} = (\% \text{ at } 0) \times 0 + (\% \text{ at } 1+) \times 1 + (\% \text{ at } 2+) \times 2 + (\% \text{ at } 3+) \times 3$, as described previously. Analysis was performed on more than 3000 cells in hotspots on the slides.

IL-6 and IL-6 receptor (IL-6R) mRNA expression was visualized in FFPE sections from two iMCD-IPL and two iMCD-TAFRO cases using the ViewRNA ISH Tissue Evaluation Kit (Thermo Fisher Scientific, Waltham, MA, US). Briefly, deparaffinized lymph node sections were boiled for 10 minutes and treated with a protease solution for 10 minutes. After formalin fixation, the ViewRNA type 1 Probe Set (Thermo Fisher Scientific) against IL-6 (VA1-13526-VT) and IL-6R (VA1-11611-VT) was used to hybridize the samples for two hours. Signals were amplified by hybridization with the PreAmplifier Mix and Amplifier Mix, allowing for the specific amplification of the target-specific signal using branched DNA technology. They were then developed using Label Probe 1-AP with FastRed substrate.

Whole Transcriptome Analysis

Total RNA was extracted from the frozen specimens using the RNeasy Tissue Mini Kit (Qiagen, Venlo, Netherlands) according to the manufacturer's instructions. RNA was quantified using an Agilent 2100 Bioanalyzer (Agilent Technologies, Santa Clara, CA, United States). Following processing using the poly A method, the remaining RNAs were fragmented using a fragmentation buffer and reverse-

transcribed into cDNA with random primers. RNA sequencing was performed using the NovaSeq 6000 system (Illumina, San Diego, CA, United States)

Gene expression profiling

To extract RNA from FFPE tissue samples, we used a Maxwell RSC RNA FFPE kit (Promega Corporation, Madison, WI, USA) according to the manufacturer's instructions. Based on the whole transcriptome analysis results, a custom panel on the nCounter platform (NanoString Technologies, Seattle, WA, USA) was created that included 105 genes that were uniformly upregulated in iMCD (Supplemental Table 1) and seven housekeeping genes. RNA extracted from FFPE tissues was hybridized overnight at 65 °C with probes, processed on the nCounter prep station, and analyzed using a nCounter digital analyzer.

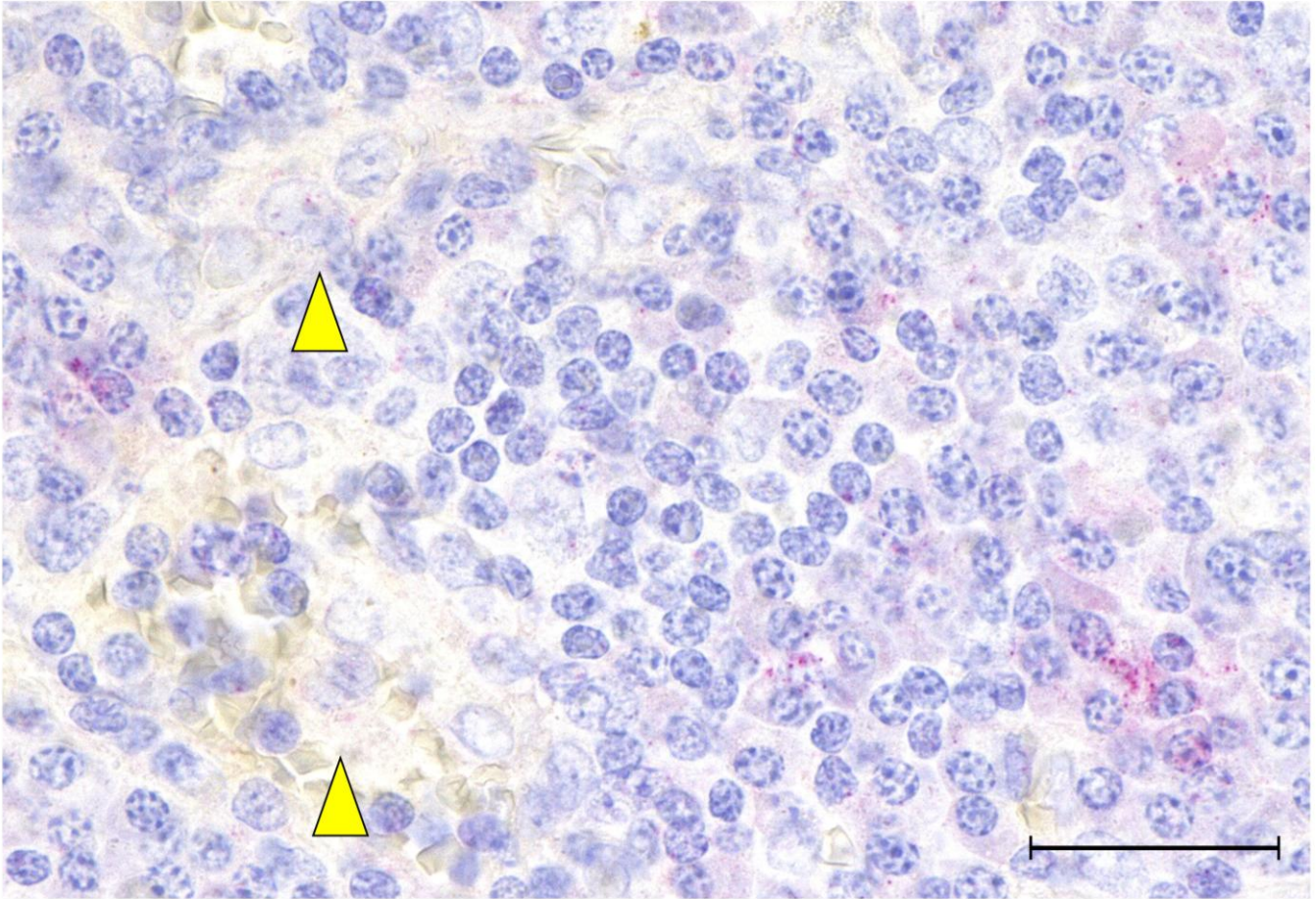
Supplemental table1. Gene sets included in custom panel

<i>ABHD14A</i>	<i>HM13</i>	<i>SDC1</i>
<i>ALDH1L2</i>	<i>HSP90B1</i>	<i>SDF2L1</i>
<i>AMPD1</i>	<i>ICAM4</i>	<i>SEC11C</i>
<i>APLP1</i>	<i>IGLL5</i>	<i>SEL1L</i>
<i>ARSA</i>	<i>INHBE</i>	<i>SERPINI1</i>
<i>ARX</i>	<i>JCHAIN</i>	<i>SIL1</i>
<i>ATAD3C</i>	<i>JSRP1</i>	<i>SLAMF7</i>
<i>ATF5</i>	<i>KCNA5</i>	<i>SLC1A5</i>
<i>B9D1</i>	<i>KRTCAP2</i>	<i>SLC35B1</i>
<i>BSC12</i>	<i>LAX1</i>	<i>SLC38A5</i>
<i>C17orf107</i>	<i>LTC4S</i>	<i>SLC3A2</i>
<i>C3orf70</i>	<i>MANF</i>	<i>SLC6A9</i>
<i>CERCAM</i>	<i>MC4R</i>	<i>SMIM1</i>
<i>CFAP54</i>	<i>MEI1</i>	<i>SMOX</i>
<i>CHAC1</i>	<i>MSLN</i>	<i>SMPDL3B</i>
<i>CHPF</i>	<i>MZB1</i>	<i>SPAG4</i>
<i>CLDN14</i>	<i>NUCB2</i>	<i>SPCS2</i>
<i>CNKSRI</i>	<i>OVOL3</i>	<i>SRM</i>
<i>COMTD1</i>	<i>P2RX1</i>	<i>SSR4</i>
<i>CRELD2</i>	<i>PDK1</i>	<i>STARD5</i>
<i>CRYBA4</i>	<i>PIM2</i>	<i>TAS1R3</i>
<i>CTH</i>	<i>PLPP5</i>	<i>TECR</i>
<i>CYBA</i>	<i>PODXL2</i>	<i>TMEM125</i>
<i>DCC</i>	<i>PPCDC</i>	<i>TMEM208</i>
<i>DERL3</i>	<i>PRDMI</i>	<i>TMEM238</i>
<i>DNAJB9</i>	<i>PRDX4</i>	<i>TP53INP1</i>
<i>DNAJC1</i>	<i>PRKCG</i>	<i>TPTE2</i>
<i>ELL2</i>	<i>PRSSI6</i>	<i>TRIM55</i>
<i>ERLEC1</i>	<i>PTP4A3</i>	<i>TSPAN1</i>
<i>FCRLB</i>	<i>QPCTL</i>	<i>TXNDC11</i>
<i>FKBP11</i>	<i>RAB26</i>	<i>TXNDC15</i>
<i>FKBP2</i>	<i>RABAC1</i>	<i>TXNDC5</i>
<i>GGT1</i>	<i>RPN2</i>	<i>WIP1</i>
<i>GNB3</i>	<i>RRBP1</i>	<i>XBP1</i>
<i>HID1</i>	<i>SCAMP5</i>	<i>ZBP1</i>

Supplemental Table2: Clinical findings of iMCD-NOS

No.	iMCD subtype	Age	Sex	(T) Thrombocytopenia ($<10^9/μl$)	Plet (* $10^4/μl$)	(A) Anasarca (Pleural effusion, ascites, or subcutaneous edema)	(F) Fever or hyperinflammatory status (Fever $\geq 37.5^{\circ}C$ or CRP ≥ 2.0 mg/dL)	(R) Renal insufficiency (eGFR ≤ 60 , Cre >1 mg/dL (F), >1.3 mg/dL (M), or renal failure necessitating hemodialysis)			Reticulin fibrosis	(O) Organomegaly (lymphadenopathy in two or more regions, hepatomegaly, or splenomegaly)	
								CRP (mg/dL)	eGFR (mL/min/1.73 m ²)	Cre (mg/dl)			
1	NOS	49	F	-	36.6	+	+	3.21	-	82	0.6		+
2	NOS	51	F	-	24.1	+	+	29.4	+	54.7	0.86	+	+
3	NOS	49	F	-	35.8	+	+	4.1	-	104.7	0.48	-	+
4	NOS	74	M	-	22	+	-	0.9	-	N/A	1.17	N/A	+
5	NOS	49	M	-	12.2	+	+	6	+	35.1	1.72	N/A	+
6	NOS	54	F	-	40.4	-	+	7.26	+	46.6	0.98	N/A	+

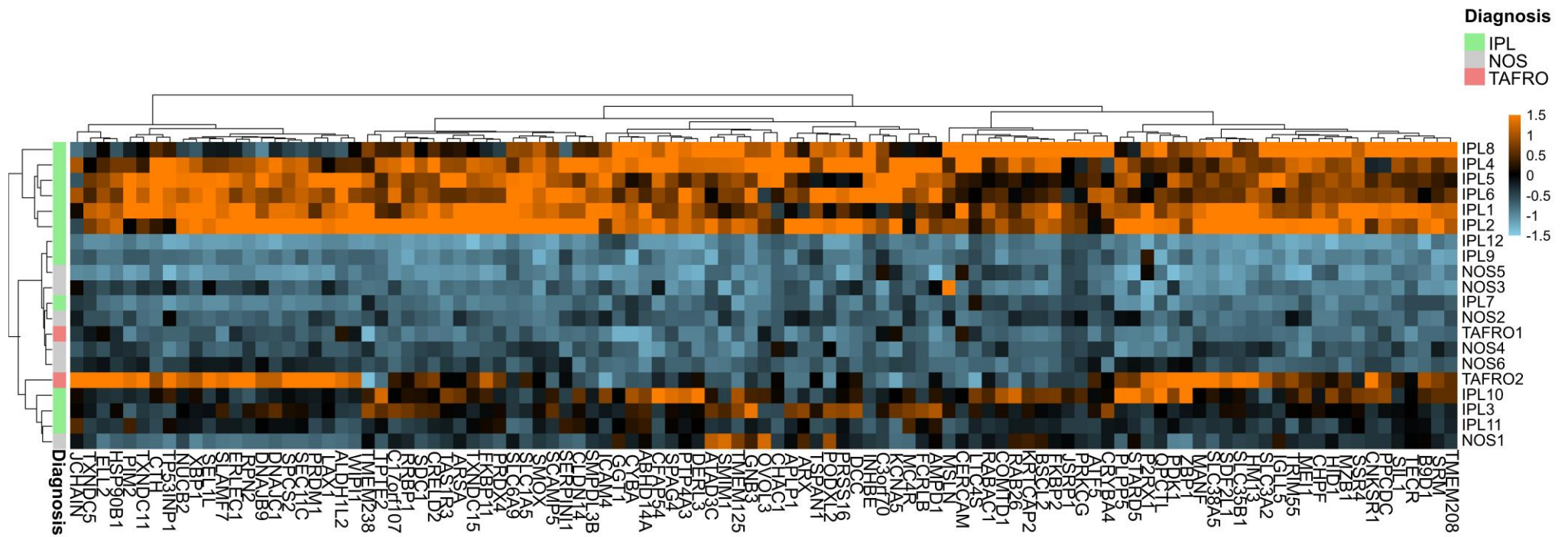
The reference considered was the laboratory data before the lymph node biopsy. The thresholds for each data point are determined based on the iMCD-TAFRO consensus criteria [31]. iMCD-TAFRO was defined as meeting at least four clinical criteria (thrombocytopenia, anasarca, fever/hyperinflammatory status, and organomegaly), renal dysfunction or reticulin fibrosis, and pathological criteria for lymph nodes. Patient 3 presented with renal failure and did not require hemodialysis.



Supplemental Figure 1: In situ hybridization of IL-6 in iMCD-IPL

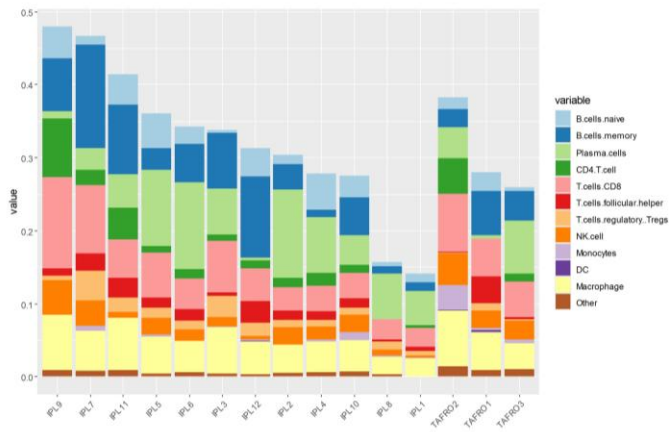
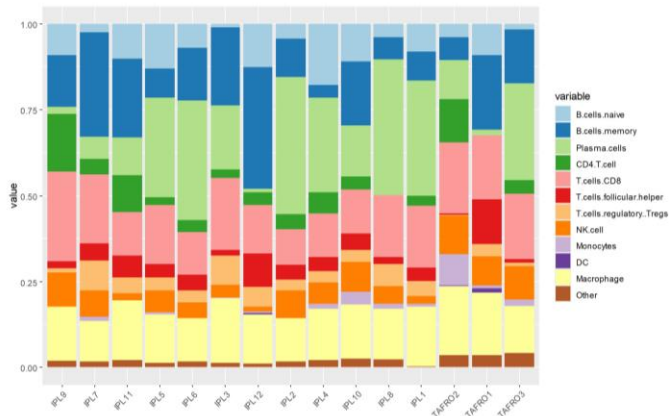
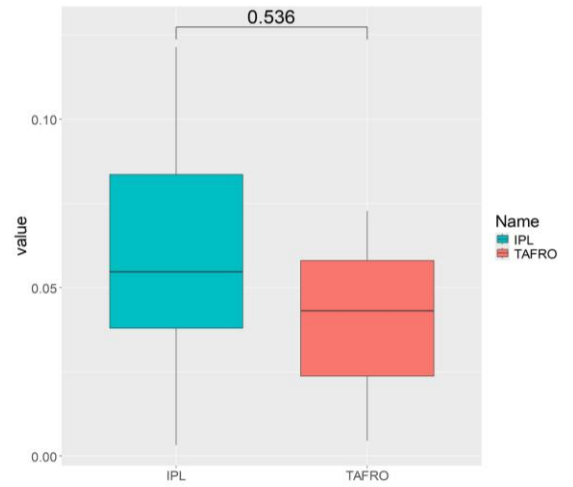
The signals of IL-6 mRNA were slightly detected in vascular endothelial cells (yellow arrowheads). These signals were weaker than those in plasma cells of iMCD-IPL (Figure 4A) and vascular endothelial cells of iMCD-TAFRO (Figure 4B).

Scale bar = 50 μ m.



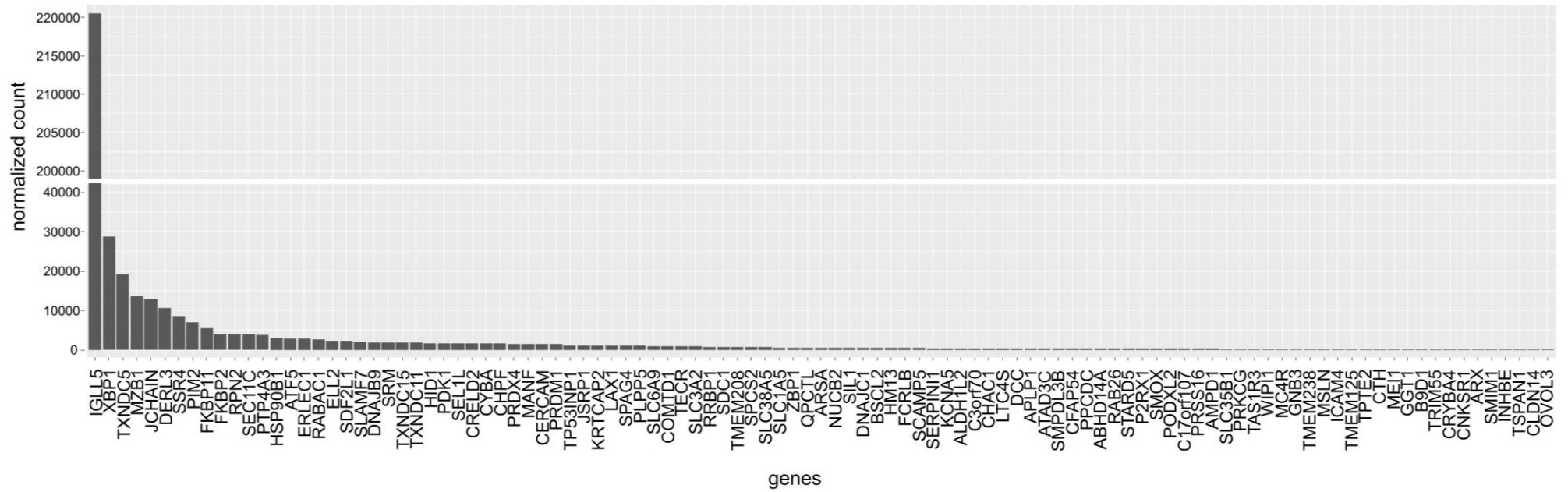
Supplemental Figure 2: Whole transcriptome analysis in iMCD subtypes

Results of clustering analysis focused on the iMCD cluster. Finally, NOS1 and TAFRO2 were excluded by gene expression patterns, and 105 upregulated genes in the iMCD-IPL group (including IPL1, 2, 4, 5, 6, and 8) were identified.

A**B****C**

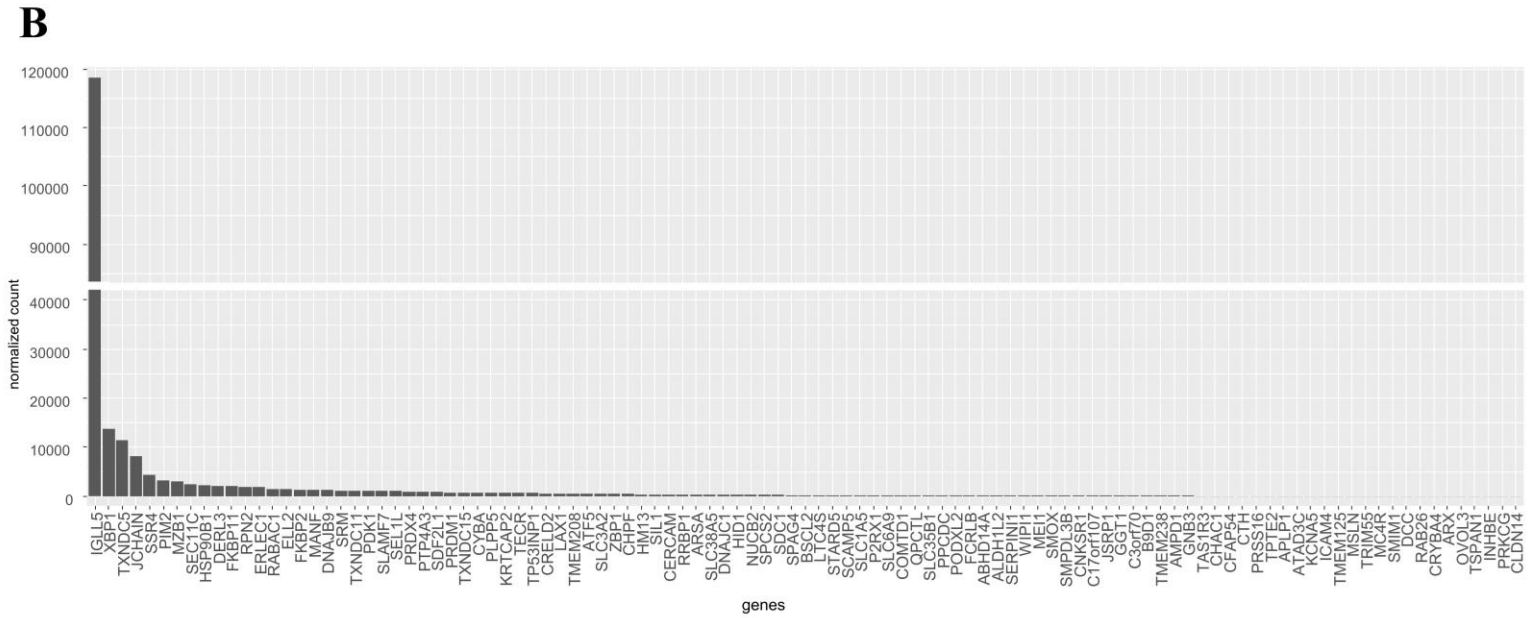
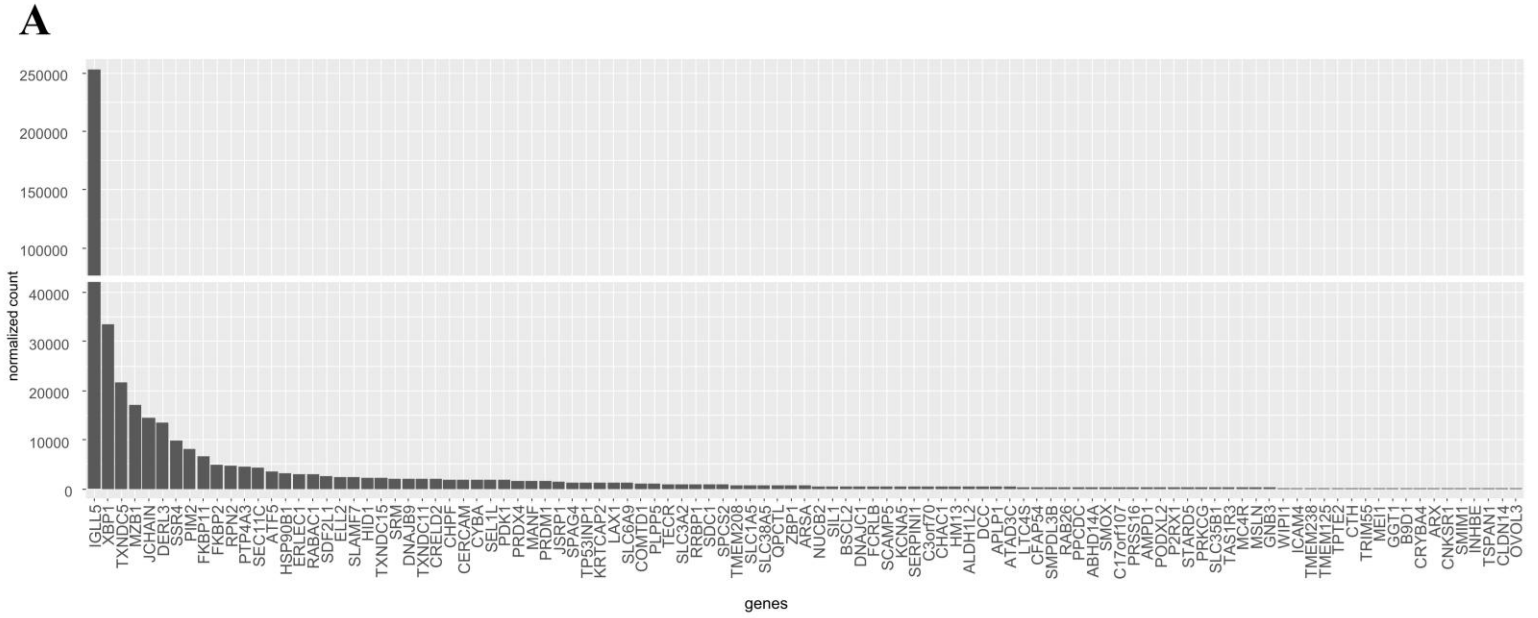
Supplemental Figure 3: Deconvolution analysis in iMCD-IPL and iMCD-TAFRO.

A, B: The cell amounts for each case were estimated using the abs mode of CIBERSORTx based on the transcripts per million (TPM) results of transcriptomic analysis. LM22 provided by CIBERSORTx was used as a reference. C: A comparison of the amount of plasma cells between iMCD-IPL and iMCD-TAFRO was performed based on the results of CIBERSORTx. No significant difference was observed in the estimated amount of plasma cells between iMCD-IPL and iMCD-TAFRO ($P=0.536$). The Mann-Whitney U test was used for the test, and $P < 0.05$ was used to measure statistical significance.



Supplemental Figure 4: Gene expression analysis in iMCD-IPL and iMCD-TAFRO using a custom panel

The normalized count was calculated for all cases and is shown in order of expression level.



Supplemental Figure 5: The average gene expression level of iMCD subtypes in the nCounter analysis.

The normalized count of cases was calculated. A: iMCD-IPL. B: iMCD-TAFRO